

DEGRADATION OF MAGNET EPOXY AT NSLS X-RAY RING

Jih-Perng Hu, Zhong Zhong, Edwin Haas, Steven Hulbert, Rodger Hubbard
Brookhaven National Laboratory Upton, New York, 11973-5000, USA
E-mail: hul@bnl.gov

Abstract

Epoxy resin degradation was analyzed for NSLS X-ring magnets after two decades of 2.58-2.8 GeV continuous electron-beam operation, based on results obtained from thermoluminescent dosimeters irradiated along the NSLS ring and epoxy samples irradiated at the beamline target location. A Monte Carlo-based particle transport code, MCNP, was utilized to verify the dose from synchrotron radiation distributed along the axial- and transverse-direction in a ring model, which simulates the geometry of a ring quadrupole magnet and its central vacuum chamber downstream of the bending-magnet photon ports. The actual life expectancy of thoroughly vacuum baked-and-cured epoxy resin was estimated from radiation tests on similar polymeric materials using a radiation source developed for electrical insulation and mechanical structure studies.

1. Introduction

The National Synchrotron Light Source (NSLS), built in the early 1980's at the Brookhaven National Laboratory (BNL) is a dedicated 2nd generation synchrotron facility [1], providing beamline users with electromagnetic synchrotron radiation emitted from dipole bending magnets as well as insertion devices (wigglers and undulators). Two closed loop storage rings, the Vacuum Ultra-Violet (VUV) ring and the X-ray ring, shown in Figure 1, are used to circulate electrons extracted from a booster ring, where electrons are accelerated from 120 MeV to 750 MeV after being injected from a klystron-pulsed 120 MeV linear accelerator (thermionic E-gun). The electrons are further accelerated to energies of 0.8 GeV and 2.8 GeV, respectively, in the VUV and X-ray rings. Intense, collimated light (photons) peaking in the soft X-ray (VUV ring) and hard X-ray (X-ray ring) range is emitted from bending magnets on these rings, where 80 beamlines and radiation hutches have been built to facilitate experiments. The magnetic lattice of the NSLS storage rings, which steers and focuses the electrons, is the double bend achromat (DBA) design developed at BNL by the late Renate Chasman and G. Kenneth Green in the late 1970's. Since all three rings in the NSLS complex (two storage rings and one booster ring) have been operating over the past two decades to produce high-brightness synchrotron light (10^{17} ph/s/mm²/mrad²/0.1%bw from the mini-gap undulator and 10^{14} from the dipole bending magnets), many non-metallic elements surrounding the beam chamber have started degrading, as evidenced by the discoloration of magnet epoxy downstream the photon's extraction port. Using bare and lead-covered (3 mm thick, which absorbs all synchrotron radiation while allowing most *bremsstrahlung* radiation through) thermoluminescent dosimeters (TLD) placed at epoxy surface facing the beam [2], synchrotron radiation alone (>99.98% total dose) has been identified as the major cause of this material degradation. The dosimetry results also show limited *bremsstrahlung* radiation (<0.02%) implying limited off-track electrons, in agreement with operation records of long beam lifetime at the X-ray ring (≥ 12 hours).

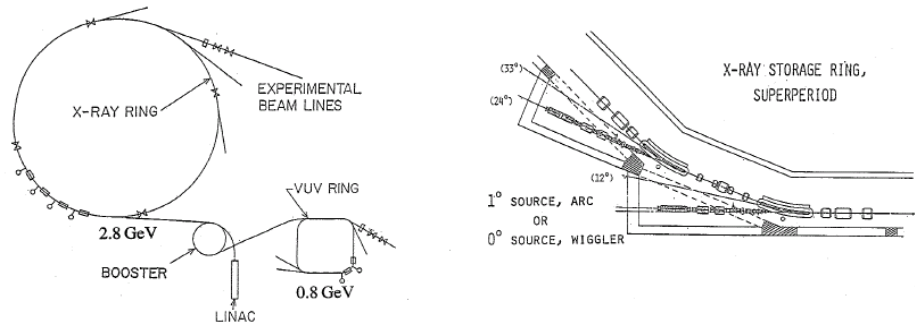


Figure 1. Schematic of the VUV-ring, the X-ring, and the Linac-to-booster ring are shown in the left. A straight wiggler and arc dipole sources in one superperiod at the X-ray ring are shown in the right.

To attenuate scattered synchrotron radiation, the free-field air spacing between the magnets and the electron beam vacuum chamber has been plugged with lead bricks and shim plates. The un-scattered photons directly streaming down the narrow chamber aperture cannot be shielded due to the absence of crotch absorber or *in vacuo* scraper, devices developed subsequent to the completion of NSLS rings (1982). Ray tracing and Monte Carlo simulations have been performed to track the photon trajectory and flux intensity at different lattice sections [3]. Our results indicate that even at the 3rd magnet in the quadrupole triplet (4-meters from the photon port) as shown in Figure 2, the integral of incident photons is still significant as compared to the un-deflected photons directly impinging onto the first quadrupole magnet next to the photon port (1.5 meters). This demonstrates that without an absorber downstream the dipole magnet to capture energetic photons scattering along the aluminum chamber wall ($E_{\text{binding}} \approx 1.6$ keV), radiation degradation of lattice components can extend a considerable distance downstream of the photon source. To evaluate the degree of degradation in terms of imparted energy (dose) from the “cloud” of scattered photons, a model simulation benchmarked with dosimeter measurements was performed.



Figure 2. Degradation of magnet epoxy shown by discoloration on the 1st quadrupole magnet in triplet can be seen from the left picture. Lattice array in one superperiod at X-ring is shown in right picture.

The NSLS design specified that all water-cooled magnet coils (multipolar magnets) be encapsulated in vacuum-baked and cured epoxy resin, thereby preventing entrapped water vapor from causing current leakage. The magnetic fields generated would then change linearly with the applied current (and number of windings per Ampere's law). Fiberglass was used during the original magnet fabrication to enhance inter-turn insulation and entire coil compaction after vacuum-impregnating each coil with low-viscosity liquid resin (Epon-828) mixed with a catalyst (Epi-cure 3140). Curing occurred initially at 150°C [4]. After days of thermo-hardening in an oven maintained at 20°C under 1 mTorr vacuum pressure, essentially void-free monolithic coils with low vapor outgassing (<0.03 Torr), high flexural strength (>13 kpsi), and large dielectric impedance (>10¹⁶Ω-cm) was produced for each magnet [5].

The life expectancy of coil epoxy (Epon resin 828) exposed to the synchrotron beam at NSLS X-ray ring was evaluated. By the use of TLDs placed at epoxy surfaces near the vacuum chamber facing the beam, the highest photon dose at the surface of the magnet operating at different beam currents was measured (≤1.2 Gy/mA-hr). The intensity of photons at quadrupole magnet in the axial and transverse directions next to the chamber septum was computed by a Monte Carlo code, where photon transport in a three-dimensional model geometry was statistically simulated. TLDs and samples of polymeric materials commonly used inside the X-ray ring were individually irradiated at the X17B1 superconducting wiggler beamline at the NSLS [6]. These experiments, under controlled and known dose, help predict the mode and timing of potential future failure of these materials under present operating conditions. The materials studied include Epon 828 (epoxy resin), Lexan (polycarbonate resin), Ultem-1000 (amorphous resin), Plexiglas (acrylics resin, Lucite), Poly-flo (polyethylene), Hytron (polyurethane-coated polyester), Micarta (linen-backed phenolic resin) and G-10 (glass-laminated phenolic resin). Through comparison with updated data published by CERN [7], the consistent portion will be referenced for the design of magnets to be used in the proposed 3 GeV, 3rd generation NSLS-II [8], which will generate photons a few orders of magnitude brighter (~10²¹ph/s/mm²/ mrad²/0.1%bw) than are being generated at NSLS.

2. Epon Resin Formation and Curing

The choice of epoxy resin as coil insulator was primarily based on its strong adhesion to metal, high tolerance to radiation, and superior dielectric insulation properties. To ease mold resin flow under vacuum (≤1 mTorr) as depicted in Figure 3, the Chevron's commercial-grade, low-viscosity, radiation-resistant liquid resin Epon-828 with low viscosity (<115 poises at ~20°C) was selected.

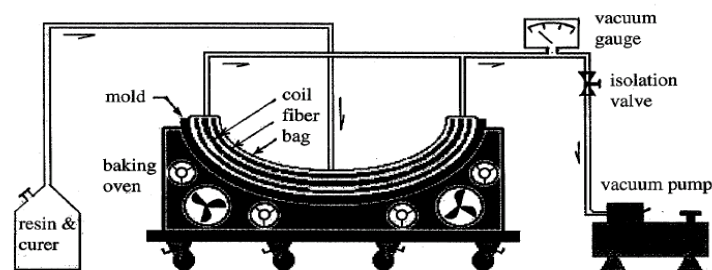


Figure 3. Sketch of vacuum impregnation of magnet coil and glass-fiber cloth in a mold (bottom half) filled with epoxy resin pumped via vacuum pipe. Air-cooled oven used for epoxy baking and curing.

The typical procedure to manufacture the 800-series Epon product begins with condensation of difunctional bisphenol-A and epichlorohydrin monomers, using an alkaline catalyst such as

sodium hydroxide (NaOH). The stoichiometric formula of reacting monomers and resulting polymer is shown in Figure 4.

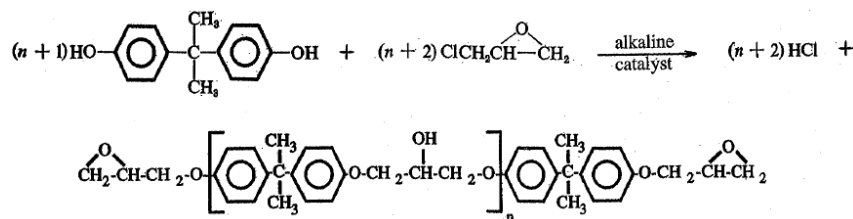


Figure 4. Chemical balance of reacting monomers bisphenol-A ($n+1$) and epichlorohydrin ($n+2$), and resulting polymer epoxy resin (bottom). Alkaline catalyst was used to boost the condensation reaction.

The viscosity and flow of the epoxy varies according to the degree of polymerization ($0 < n < 10$, which yields low molecular weight $< 3,100$ of the recurring compound $-[\text{R}]_n-$ plus two epoxy end-groups $-\text{O}-$), thus during the time that the coil initially starts to cure, the Epon resin remains primarily in a liquid state. The best overall performance of the Epon resin for a magnet coil is obtained from a 50-50 blend by weight, of Chevron's Epon-828 resin with curing agent Epi-cure 3140. The amber-colored resin curer is a commercial-grade, room-temperature liquid solution that is formed with a 16-84 mix by weight of highly-volatile reactant triethylene tetramine (TETA) and highly-flexible catalyst fatty-acid polyamides. The two-dimensional unit structure of the TETA and polyamides prior to their mixing into an active curer can be individually expressed by a series of carbon-centered clusters as depicted in Figure 5.

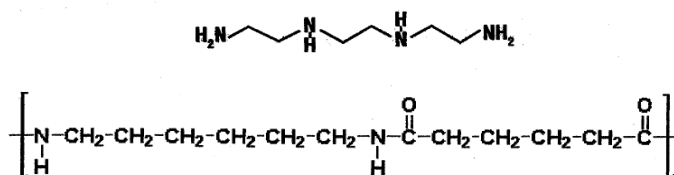


Figure 5. The unit chemical structure of linear triethylene tetramine (TETA) and acidic polyamide (e.g. nylon 6-6) prior to their mixing into an active curer of the Epon resin are individually shown above.

Curing of the Epon resin with Epi curer is an exothermic process, involving three-dimensional cross-linking and multiple epoxy-hydroxyl end-group reactions. As the epoxy cures, heat is released (~ 59 kcal/mole, 45-min at 20°C). This is shown schematically in Figure 6. After curing, the long-chain polymers are fully cross-linked and the coil epoxy becomes hard, physically rigid, and chemically inert [9], thereby meeting the design criteria for the NSLS magnet components [10].

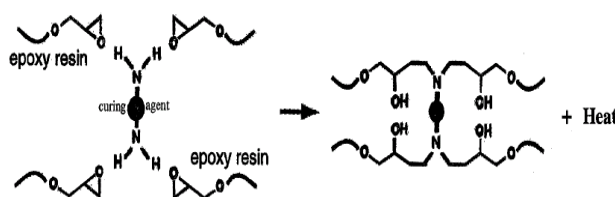


Figure 6. Curing of the epoxy resin involving 3-D networking and epoxy-hydroxyl end-group reactions.

To ensure that strength of magnetic field is not adversely affected by the epoxy, standard magnetic and thermal measurements on each of the assembled magnets were performed [11], at the same air-cooled or water-cooled conditions that would be encountered in actual operation. The highest field strength at the maximum allowable temperature of the Epon resin (which softened at 105°C and distorted at 140°C) was then evaluated to characterize the magnet. No radiation testing of the magnet epoxy was performed, primarily due to tight operating budgets, schedules, and lack of available man-power. A qualitative analysis of epoxy degradation using computer code modeling coupled with TLD measurement is presented here as a first cut of a long-term radiation study. Since degradation of commonly used polymeric materials has been extensively studied and conservatively analyzed by CERN [7], cross comparison can be made through appropriate scaling.

3. Monte Carlo Simulation

Synchrotron radiation distributed along the ring's axial- and transverse-direction at quadrupole magnet downstream of the photon port was calculated, using Monte Carlo based particle-transport code MCNP [12]. The MCNP is a general-purpose Fortran-compiled software package that can be used to model any single-particle motion or coupled electron-photon transport in a three-dimensional geometry consisting of different material regions. Components such as ring magnets are generally simplified (coil symmetry is used, the magnet assembly is compacted, and the materials are considered homogeneous). Using MCNP, the model geometry included a straight rectangular channel (the beam vacuum chamber) and a coaxial cylinder (the ring magnet) consisting of contiguous concentric regions as depicted in Figure 7.

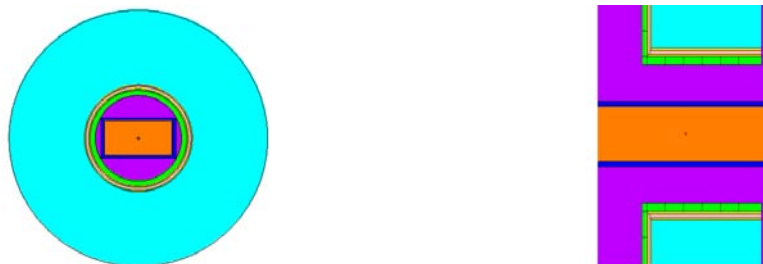


Figure 7. The circular cross-section in MCNP code two-dimensional plots shows concentric regions of magnet steel (outer ring), copper coil, water channel, and epoxy resin (inner ring) surrounding the rectangular chamber that separates outside air from inner vacuum. The right figure shows symmetric poles of magnet in model where epoxy region was segmented to ease peak dose and distributed flux estimation.

A point source of photons simulating the flux spectrum from 2.8 GeV electrons traversing a 1.36 Tesla bend, as shown in Figure 8 (red curve), was setup to generate particle history (random walk) along the beam path, starting from the center of dipole magnet photon port down to the symmetric axis of the first quadrupole magnet (~2 meters in length). In view of the directional nature of the photon beam, a forward-biased source instead of an isotropic source (the default) was defined.

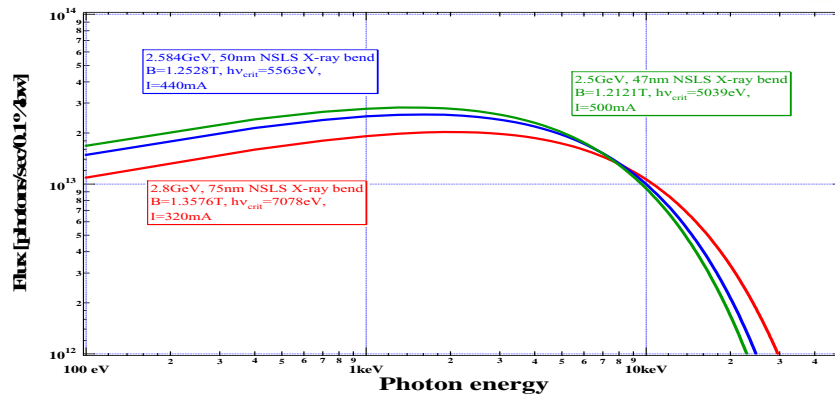


Figure 8. Photon flux spectrum of 2.8 GeV electron energy and 1.36 Tesla bending field at X-ring was simulated to setup the MCNP source term, which covers the energetic photons up to 200 keV range.

Homogeneous nuclide composition was assumed in each material region of the model such that average interactions between the incident photons and residing nuclides could be efficiently tallied. Continuous nuclide cross-section libraries were called to process the coherent and incoherent scattering of photons crossing different material regions with varying energy and colliding angles. To enhance particle transport through model geometry using the scheme of space splitting, a set of weighting factor obtained from preliminary code runs were assigned to each of the segmented regions for history tracking.

For the purpose of ensuring quality output, termination of the MCNP run for each case study was determined by the tally's confidence indicators instead of total running time or particle's history size (the default). When the relative error of the population mean falls to within $\pm 5\%$ of one sigma ($1-\sigma$), MCNP code tallies were registered and the simulation was terminated. After normalizing to the highest dose on magnet epoxy where each TLD was placed (1.187 Gy/mA-hr), average photon doses deposited on the magnet pole surfaces along and traverse to the electron beam axis can be obtained as shown in Figure 9.

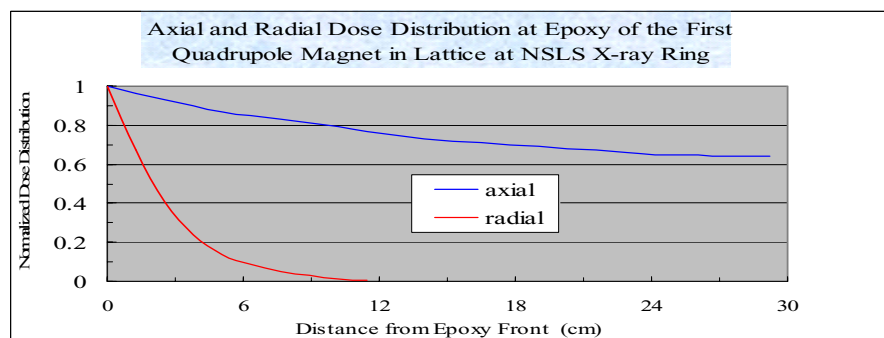


Figure 9. The normalized photon dose on magnet epoxy along the ring's axial- and radial-direction. A Monte Carlo-based code was used to model the ring lattice from dipole photon port to quadrupole magnet.

4. Experimental Method at the Superconducting Wiggler Beamline (X17B1)

To validate the photon dose measured at quadrupole magnet and to compare the radiation resistance of polymeric materials used along the ring, bare TLD chips (Li_6F - and Li_7F -chips) and organic-based thermoset and thermoplastic specimens (resin, phenoplast) were

individually irradiated at a beam port within the experimental hutch. For the purpose of expediting the specimen irradiation to build a large database for material degradation studies, the superconducting wiggler (SCW) beamline X17B1 was used. This beamline provides the highest photon beam power and radiation level of all the NSLS beamlines, more than 100 times that from a dipole magnet beamline. Commissioned in 1984, the X17B1 beamline was designed for high-energy X-ray scattering, crystallography, and material studies using a graphite-filtered photon beam extracted from a 7-pole, NbTi-SCW [6]. This high-energy X-ray insertion device is shown in Figure 10.

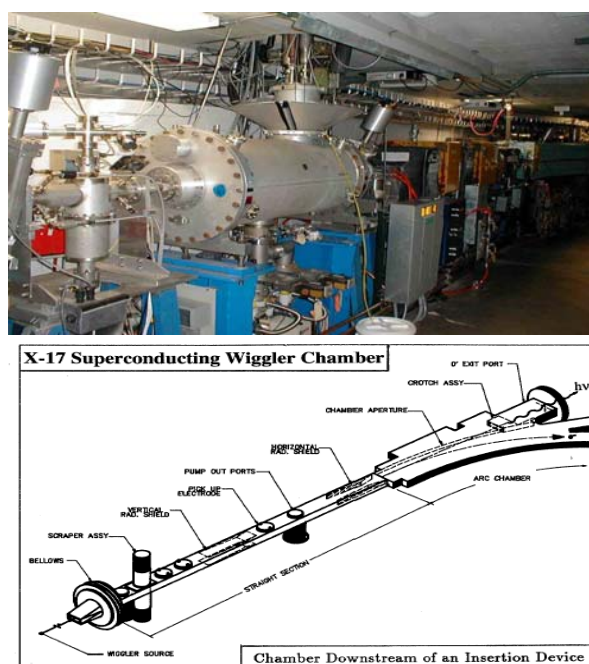


Figure 10. The 7-pole, NbTi-superconducting wiggler installed at X-ring is shown in left. The wiggler downstream straight section, arc chamber, scraper, septum, aperture, port, and shield are shown in right.

The X-ray ring electron beam typically operates at 300 mA and 2.8 GeV, with the SCW ramped to a 4.2 Tesla field. At this operating current, energy, and magnetic field, the wiggler produces a spectrum of photons up to 200 keV ($E_c=21.9$ keV) at the beamline target [13]. When the beamline monochromator is used for monochromatic beam experiments requiring high beam focusing ($40 \rightarrow 0.5$ mm horizontal width in 5.6-m focal length), the energy and flux density of photons are 67 keV and 10^{11} ph/s, respectively. For this experiment, the monochromator was moved out of the path of the white beam and an aluminum filter of 6.5-mm thick was used to attenuate the low-energy part of the beam spectrum. The thickness of the filter was chosen so that a) the energy spectrum of the filtered beam is similar to that the ring magnet epoxy is subjected to, b) the heat load of the beam on the sample is minimized so as to measure the net effect of radiation damage. Figure 11 shows the spectra of the white beam incident to the hutch, and that after the filter. The mean energy of the filtered beam is 51.4 keV, which has sufficiently high penetrating power to ensure uniform dose rate throughout the typical sample thickness of 3-10 mm. The water-equivalent dose rate for typical ring current of 200 mA is 2300 Gy/s (2×10^8 Gy for 24 hours of continuous irradiation). For polymeric materials primarily formed in repeating organic compounds ($-\text{[CH}_2\text{]}_n-$) and functional end-groups that are less resistant to the high-energy gamma rays (>200 keV), the use of hard X-rays (20-100 keV) from the filtered wiggler white beam for sample irradiation is deemed adequate and efficient.

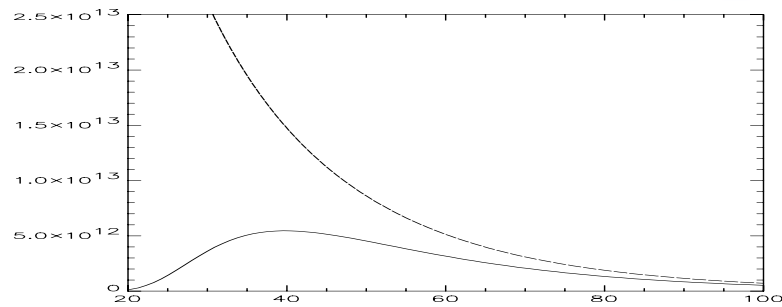


Figure 11. The spectra of the white beam incident to the hutch (dashed line), and that after the 6.5 mm aluminum filter (solid line).

The polymer specimens or TLD chips were placed in the beam path at a distance of 1.5 meters from the beamline and aluminum filter (6.5-mm thick) at the front of the lead-covered experimental station, as shown in Figure 12 (a). Stepping-motor driven translation stages were used to position a universal sample holder which firmly supports the specimen during its two-dimensional motion perpendicular to the incoming photon beam. A computer-controlled shutter constructed of 10-mm Ta was used in front of the sample to allow irradiation of each spot for a preset time.

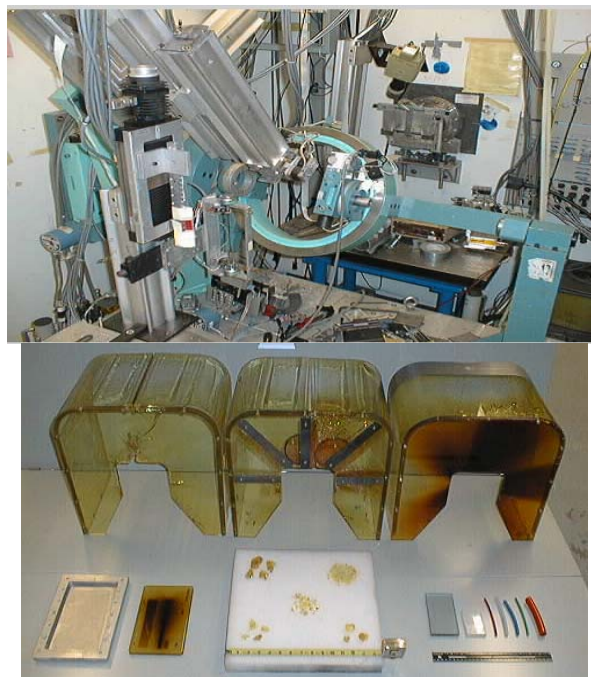


Figure 12. (a) Left picture shows the polymer specimen (white) held on a universal sample holder in the X17B1 hutch facing the incoming beam (square center). (b) Right picture shows three degraded Lexan covers used to protect electric busbars. Front-left is the mold fixture used to make the epoxy test plate (irradiated), and front-right is hoses and samples to be irradiated. At front-middle are cracked Lexan pieces.

To control the sample motion, the shutter, and to monitor the incoming beam during specimen irradiation, a Linux PC running SPEC and a CAMAC data acquisition system was used [6]. Different locations on the specimen are used for progressively longer irradiation time (double at every data point). The shutter was automatically closed during transition from one data point to the next. The total dose received is calculated using an IDL dose calculation program and the known white beam spectrum and filter thickness. As the white beam (6-mm wide by 3-

mm high) exposure increased, an increasing discoloration caused by double-bond formation and free-electron trapping in the specimen appeared [7]. A collimated diode-laser was used to examine the light transmitting through the specimen. The apparent discoloration was therefore related quantitatively to the radiation dose received. This information is then used to estimate the dose already received by the ring magnet epoxy. When the laser light was fully blocked through dark discoloration after high dose collection, the specimen deterioration was then evaluated in terms of the permittivity (dielectric constant) measured (a dimensionless parameter). Since the polymers' electric insulation capability is of major interest, a digitized RLC-meter [14] was used to help identify the dose from photons that would cause irreparable scission in the polymer chain (slump of permittivity) and potentially lead to dielectric breakdown of the polymer structure (permittivity→1). Referring to these "yielding" and "failure" threshold points of the specimen [15], the expected life of polymer under photon radiation was estimated.

5. Results and Conclusions

When the X-ray ring at NSLS was upgraded from an electron energy of 2.58 GeV to 2.8 GeV in 2000, the scattered synchrotron radiation passing through a small chamber aperture increased to six times higher than that encountered at 2.58 GeV [16]; thus material degradation was expedited. As shown in Figure 12 (b), the electric busbar covers made from Lexan (polycarbonate resin) showed unacceptable damage after three years of use due to back-scattered photons from the lead bricks stacked around the dipole magnet photon ports. The embrittlement of Poly-flo (polyethylene) cooling water hoses is another example showing the dose effect from scattered synchrotron radiation. These hoses are now replaced every two years with high radiation-resistant Hytron hose (polyurethane-coated polyester). The standard spacer and insulating materials used at lattice magnets, G-10 (glass-laminated phenolic resin) and Micarta (linen-backed phenolic resin), discolored severely after extended exposure to the photon beam also raised concerns at NSLS.

The ability of polymers to withstand synchrotron radiation as estimated from permittivity measurements is shown in Table 1. The listed lower and upper dose limits are those corresponding to the scaled RLC-meter readings on the tested specimen exhibiting irreparable scission (slump of permittivity) or breakdown of the polymeric structure (permittivity→1) after exposure to the filtered synchrotron beam at X17B1.

Table 1. Photon dose range obtained from measured permittivity (scission-to-breakdown) of the polymer specimens versus reported data by CERN [7], based on scaling to meet same conditions

Polymer Specimens (irradiated at X17B1)	Thermosetting versus Thermoplastic ^(#) Resin	Dose Range measured by Permittivity (Gy) *	Dose Range reported by CERN (Gy) *
Plexiglas (Lucite)	acrylic resin ^(#)	$1 \times 10^4 - 1 \times 10^5$	$7 \times 10^3 - 1 \times 10^5$
Lexan (no fiberglass)	polycarbonate resin ^(#)	$5 \times 10^5 - 6 \times 10^6$	$3 \times 10^5 - 3 \times 10^6$
Ultem-1000 (pure)	amorphous resin ^(#)	$4 \times 10^7 - 1 \times 10^8$ *	(no data)
Poly-flo (not coated)	polyethylene	$8 \times 10^4 - 6 \times 10^5$	$1 \times 10^5 - 5 \times 10^5$
Hytron (coated hose)	polyurethane on polyester	$4 \times 10^6 - 8 \times 10^7$	$2 \times 10^6 - 6 \times 10^7$
Teflon (TFE or FEP)	polytetrafluoroethylene ^(#)	$4 \times 10^4 - 9 \times 10^5$ (TFE)	$2 \times 10^4 - 8 \times 10^4$ (FEP)
G-10 (standard)	phenolic (glass laminated)	$5 \times 10^7 - 1 \times 10^8$ *	$6 \times 10^7 - 1 \times 10^8$ *
Micarta (standard)	phenolic (linen backed)	$2 \times 10^7 - 1 \times 10^8$ *	$1 \times 10^7 - 1 \times 10^8$ *
Epon Resin (cured)	epoxy resin	$3 \times 10^6 - 6 \times 10^7$ (Epon 828)	$1 \times 10^5 - 5 \times 10^6$ (generic)

(* At level of 10^8 Gy, most of the main polymer chains are ruptured and the side chains are decomposed)

In general, CERN's report refers to products generically instead of by a more commonly-known commercial product name [7]. The strength of polymeric materials used at the NSLS was deemed adequate under previous 2.58 GeV operating energy. At 2.8 GeV the life of many non-metallic materials diminishes, primarily due to a significant increase in photon dose from the high-energy end of the synchrotron radiation spectrum (≥ 20 keV in Figure 8). For the magnet epoxy (Epon resin 828) surrounding the pole pieces downstream of the dipole magnet photon port at NSLS' rings, the predicted remaining life is ≤ 7 years, prompting a review of the epoxy in all magnets, with priority being given to the quadrupole magnets in the lattice. After seven more years of nearly continuous operation at 2.8 GeV, it is expected that the epoxy resin would be degraded to an unacceptable level. It is noted that, due to the use of inorganic fiberglass tape that is capable of maintaining its integrity even after a long-term, continuous exposure of synchrotron radiation, the degraded coil epoxy will still be held in place. However, the mitigating effects provided by radiation-resistant fiberglass tape were not taken into account, since the possibility that water vapor may quickly permeate the degraded epoxy and eventually cause an electrical short at the magnet still exists.

Results from this study provide the basis to estimate current dose exposure received by polymers at various locations around the ring, and guidelines to predict the remaining lifespan of the polymers repeatedly exposed to the synchrotron radiation along the storage ring. In planning any ring energy upgrade, the original design of the magnet assembly needs to be revisited since the dose accumulated from the increased photon scattering would be significant, and is expected to increase as the fourth power of the beam energy.

6. Acknowledgements

The authors are grateful to C. Ochamphugh of the Landauer, Inc. for her collaborative service on the TLD and heating test on dosimeter chips. Consultations with W. Caliebe, T. Dickinson, M. Fulkerson, P. He, S. Kramer, A. Pendzick, R. Scheuerer, J. Skaritka, and J. Tuozzolo of the BNL are also gratefully acknowledged. This research was supported by the U. S. Department of Energy, under the contract DE-AC02-98CH10886.

7. References

- [1] National Synchrotron Light Source (NSLS) and proposed 3 GeV, new light source (NSLS-II). Surf <http://www.nsls.bnl.gov> for details of the rings and beamlines, 2004.
- [2] Landauer's TLD and controlled badge. Landauer, Inc., 2 Science Rd., Glenwood, IL, 60425, 2003.
- [3] Galayda J., POISSON 2-D mesh modeling for the NSLS magnets design, 1978.
- [4] Epon resin 828 and Epi-cure 3140, developed by the Chevron Oil Company and distributed by the Resolution Performance Products, PO Box 4500, Houston, TX, 77210, 2004.
- [5] Miles D. C. and J. H. Briston, Polymer Technology (ISBN 0-8206-0255-8), Chem. Pub. Co., 1979.
- [6] Thomlinson W., D. Chapman, N. Gmür, and N. Lazarz, The Superconducting Wiggler Beamport at the NSLS. Nucl. Inst. & Meth. in Phys. Res. A(266), P.226-233, Elsevier Sci. Pub. B.V., 1988.
- [7] Van de Voorde M. H., Effects of Radiation on Materials and Components, CERN 70-5, 1970; and Tavlet M., A. Fontaine, and H. Schönbacher, Compilation of Radiation Damage Test Data, Part-II, 2nd ed., Thermoset and Thermoplastic Resins, Composite Materials, CERN 98-01, 1998.
- [8] NSLS-II: A Bright New Light Source. Surf <http://www.nsls2.bnl.gov> for details, 2004.

- [9] Gross S., R. Cassel, and T. Mattison, Development of Epoxy Potting for High Voltage Insulation at SLAC, Particle Accelerator Conf. (PAC 1991), p. 2334-2336, IEEE pub. (0-7803-0135-8/91), 1991.
- [10] NSLS Design Handbook (revised on 9/01/1978). Brookhaven National Lab, Upton, NY, 11973, 1978.
- [11] Hu J.-P., W. Casey, D. Harder, S. Pjerov, G. Rakowsky, and J. Skaritka, The Mechanical and Shielding Design of a Portable Spectrometer and Beam Dump Assembly at BNL's Accelerator Test Facility (BNL-69398), MEDSI02, p.23-29, Argonne National Laboratory, 2002.
- [12] Briesmeister J. F. (ed.), MCNP - A Monte Carlo N-Particle Transport Code (ver. 4B2), LA-12625-M, developed by the Los Alamos Nat. Lab., and distributed by the Oak Ridge Nat. Lab., 1997.
- [13] Zhong Z. and P. Montanez, X17B2 and B3 Beamlines – Prepared for the NSLS Beamline Safety Review. BNL-NSLS Internal Report, 2003.
- [14] Dielectric Constant, surf <http://www.Ptli.com/testlopedia/tests/D150Dielectric.asp> for system usage, 2004.
- [15] ASTM Standards for testing, surf <http://www.astm.org/cgi-bin/SoftCart.exe/BOOKSTORE/COMPS/CONTENTS/70.html?L+mystore+vfeh7766> (2004).
- [16] Dickinson T., Synchrotron Radiation Sources - A Primer (H. Winick ed.), page 450, World Sci., 1994.